# High resolution dual frequency observations of 3C205 - Tighter constraints on radio source mechanisms

Lonsdale, C.J.; Barthel, P.D.

Astron. Astrophys. 135, 45–52 (1984)

ASTRONOMY AND ASTROPHYSICS

# High resolution dual frequency observations of 3C205. Tighter constraints on radio source mechanisms

**C. J. Lonsdale**[1,*] **and P. D. Barthel**[2]

[1] Nuffield Radio Astronomy Laboratories, Jodrell Bank, Macclesfield, Cheshire SK11 9DL, England
[2] Leiden Observatory, P.O. Box 9513, NL-2300 RA Leiden, The Netherlands

Received October 3, accepted October 24, 1983

**Summary.** Radio maps of 3C205 are presented at 18 cm and 6 cm wavelength, with angular resolutions of between 0.″25 and 0.″025. These maps reveal the presence of a very compact hotspot in the southern lobe of the source ($<0.''015 \times 0.''03$), as well as a very high degree of alignment between the hotspots and the radio core. The southern radio lobe is shown to have a complex morphology which is suggestive of outflow of material from the abovementioned compact feature. Also, there is a marginal detection of an elongation of the core component in a direction different from that of the source axis.

These data are discussed in the context of both a beam model, and a plasma cloud type model, leading to constraints which are interesting, but different in each case. In the beam model, it is shown that a very high efficiency is required for conversion of jet energy to relativistic particle and magnetic field energy. Also, constraints are set upon the behaviour of the ejection direction. In the cloud model, it is argued that the hotspot is probably located at the stagnation point in the bow shock flow around the cloud, thus allowing limits to be set on the inhomogeneity of the external medium, and the timescale of fluctuations of the ejection direction. In either model, the hypothesis of outflow from the compact hotspot necessitates very dense material ($n>1\,\mathrm{cm}^{-3}$) in the vicinity of the hotspot, thus raising the possibility of optical emission being present.

**Key words:** quasars – radio source structure – radio source formation

## 1. Introduction

The properties of radio sources at high redshift are at present poorly determined, due to the fact that high redshift sources are both weak and of small angular size relative to similar sources at low redshift, and are thus difficult to observe in detail. The resulting gap in our knowledge of the radio source phenomenon seriously hampers our analysis of the cosmological evolution of these objects, and also obscures phenomena which may be peculiar to sources in the high $z$ environment. One example of the latter is the apparent abundance of extremely compact, powerful hotspots in the outer lobes of such sources (e.g. Kapahi and Schilizzi, 1979; Barthel, 1983). Recently, the authors embarked on a project designed to use the new capabilities of MERLIN and the European VLBI network (EVN) to overcome some of the abovementioned observational difficulties, and to start to fill the gap at high redshift. A sample of high-redshift radio loud quasars with steep radio spectra was defined and for those sources which appeared sufficiently strong and compact to be successfully observed using MERLIN, a program involving 18 cm and 6 cm MERLIN plus 18 cm EVN observations was initiated. Details of the project aims and selection of sources may be found in Barthel and Lonsdale (1984). A total of 12 sources are presently under study, and as the observations progressed, it immediately became apparent that 3C205 was of special importance.

3C205(0835+580) is identified with an $18^{m}$ quasar of redshift 1.534 (Wyndham, 1966; Schmidt, 1968), and had previously been observed at 5 and 15 GHz with the Cambridge 5 km telescope by Pooley and Henbest (1974) and Laing (1981). The source is a triple, of overall extent $\sim 17''$ ($\sim 85\,\mathrm{kpc}$[1]), and (at 5 GHz) unequal flux densities in the outer lobes. The stronger southern component is $\sim 14\%$ polarised, with the $E$ vector in p.a. 72° (Pooley and Henbest, 1974) and also shows significant correlated flux density on baselines of up to 3 Mλ (Kapahi and Schilizzi, 1979; Barthel, 1983). We have observed the source with MERLIN at 1666 MHz and 5 GHz, and with the EVN at 1612 MHz, giving angular resolutions between 0.″25 and 0.″025. A number of remarkable features became apparent as a result of these observations, allowing constraints to be placed on the fundamental source mechanisms which are significantly more stringent than those hitherto applicable. The most important of these are the overall linearity of the source (which is good to $\sim 1$ part in 400), and the extremely compact subcomponent in the complex southern lobe. Respectively these constrain the collimation energy transport mechanism, and the hotspot formation, confinement and evolutionary processes.

In Sect. 2 we present the observations and describe the features revealed in detail, whilst in Sect. 3 the constraints on general source mechanisms are discussed.

## 2. Observations and results

### 2.1. *The* MERLIN *observations*

We observed 3C205 using six telescopes of the MERLIN array (Davies et al., 1980) at a frequency of 1666 MHz in October 1982, for a continuous period of $\sim 20$ h. The map (Fig. 1a) shows the source at a resolution of 0.″25 with a noise level of about 1 mJy. The southern hotspot complex is shown in more detail in Fig. 1b. The MERLIN 5 GHz observations were made in April 1982 using five

*Send offprint requests to:* P. D. Barthel
* Present address: Dept. of Astronomy, Pennsylvania State University, USA

1 Assuming $H_0 = 75\,\mathrm{km\,s^{-1}\,Mpc^{-1}}$, $q_0 = 1/2$

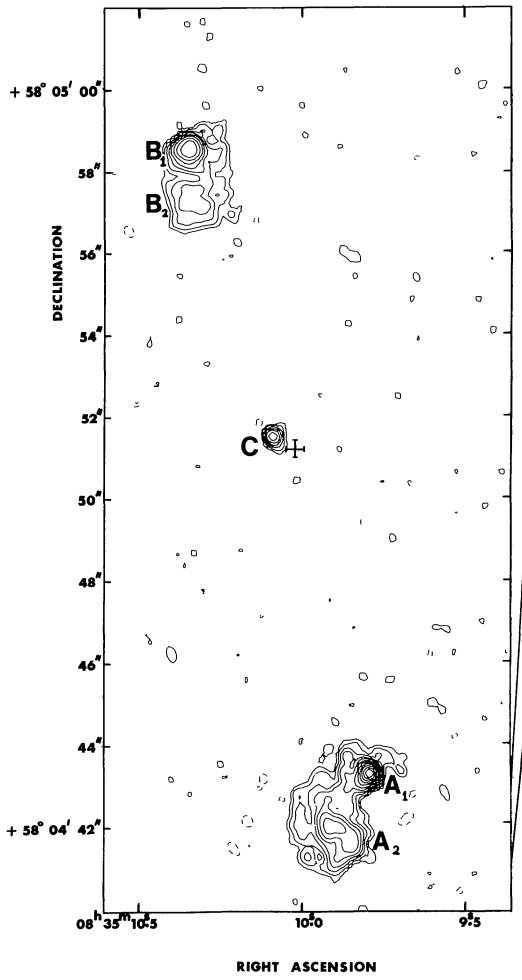


Fig. 1a

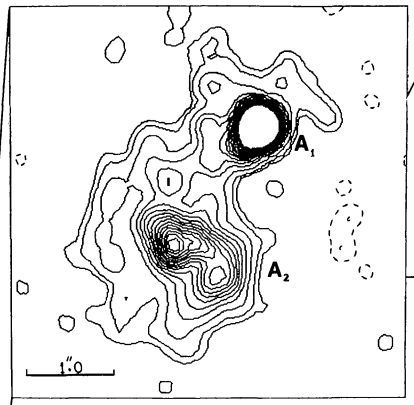


Fig. 1b

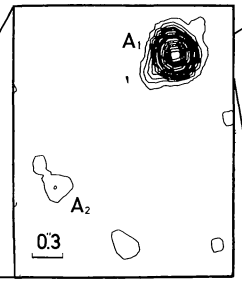


Fig. 2a

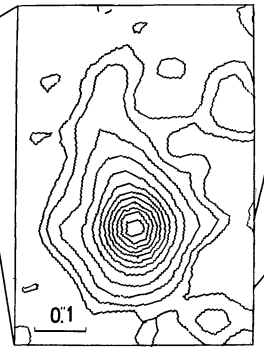


Fig. 2b

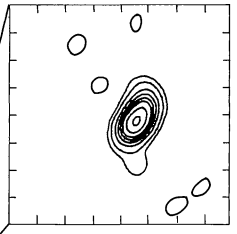

Fig. 3

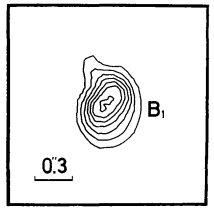


Fig. 2c

**Fig. 1a.** 3C205 at 18 cm. The restoring beam has a FWHM of 0.″25. The positional coordinates have been fixed by comparison with the 15 GHz map of Laing (1981). The cross marks the position of the quasar, with a size corresponding to the combined optical and radio positional errors. Contour levels are 1/3, 2/3, 4/3, 7/3, 4, 7, 12, 20, 32, 50, 70% of the peak brightness of 367 mJy/beam ($A_1$)

**Fig. 1b.** Southern lobe of 3C205 at 18 cm. The angular resolution is the same as in Fig. 1a, but the contour levels have been chosen to show the detailed structure in $A_2$ to best advantage. Contour levels are 1, 2, 5, 10, 15, ..., 65 mJy/beam. In this and all subsequent maps, except Fig. 3, the angular scale is indicated by a bar in the lower left hand corner

**Fig. 2a.** Southern lobe of 3C205 at 6 cm. This map was made without Defford in the array (see text), and the angular resolution is 0.″18. Note the narrow extension to the southeast of $A_1$, pointing towards the peak of $A_2$. Contour levels are 2, 4, 6, 8, 10, 12, 15, 20, 25, 30, 40, 50, 60, 70, 90% of the peak brightness of 122 mJy/beam

**Fig. 2b.** Component $A_1$ at 6 cm. With Defford included, a restoring beam of 0.″1 was used. Contour levels are 2, 4, 8, 15, 25, 35, 45, ..., 95 mJy/beam. The peak brightness is 102 mJy/beam

**Fig. 2c.** Peak of component $B_1$ at 6 cm. Resolution and contour levels are as in Fig. 2a

**Fig. 3.** Southern hotspot of 3C205 at 18 cm (EVN). A restoring beam of 25 milliarcsec FWHM was used. Tick interval is 30 milliarcsec. Contour levels are 5, 10, 20, 30, 40, 50, 70, and 95% of the peak brightness, which is 59 mJy/beam

**Table 1a.** Measured component parameters

| Component | $S_{408}$[a] | $S_{1666}$ | $S_{2700}$[b] | $S_{5000}$[c] | $S_{15000}$[b] | $\Theta_{min}$ | $\Theta_{maj}$ |
|---|---|---|---|---|---|---|---|
| | (mJy) | | | | | (″) | |
| $A_1$ | $1800\pm50$ | $660\pm15$ | $960\pm50$ | $500\pm50$ | $64\pm6$ | <0.015 | 0.035 (peak) |
| $A_2$ | $2200\pm50$ | $670\pm15$ | | | $40\pm10$ | 0.5 | 3.5 |
| $B_1$ | $1650\pm50$ | $460\pm10$ | $410\pm20$ | $190\pm20$ | $20\pm5$ | 0.3 | 0.5 |
| $B_2$ | $910\pm30$ | $145\pm10$ | | | | 0.7 | 0.7 |
| $C$ | $50\pm10$ | $55\pm5$ | | $20\pm5$ | $10\pm10$ | <0.1 | 0.1 |

The angular sizes $\Theta_{min}$ and $\Theta_{maj}$ are the half power widths after deconvolution with the beam
[a] Robson et al. (1984)
[b] Laing (1981)
[c] Pooley and Henbest (1974)

**Table 1b.** Calculated component parameters

| Component | $\alpha_{408}^{1666}$ | $\alpha_{1666}^{15000}$ | $\alpha_{2700}^{15000}$ | $L_{tot}$ (erg s$^{-1}$) | $U_{min}$ (erg cm$^{-3}$) | $T_{synch}^{5000}$ (yr) |
|---|---|---|---|---|---|---|
| $A_1$ | −0.71 | −1.06 | −1.30 | $3\,10^{44}$ | $2.3\,10^{-6}$[a] | $8\,10^{2}$[a] |
| $A_2$ | −0.85 | −1.28 | | $5\,10^{44}$ | $4.2\,10^{-8}$[a] | $4\,10^{4}$[a] |
| $B_1$ | −0.91 | | | $3\,10^{44}$ | $5.5\,10^{-8}$ | $2\,10^{4}$ |
| $B_2$ | −1.31 | | −1.76 | $3\,10^{44}$ | $4.1\,10^{-8}$ | $4\,10^{4}$ |
| $C$ | +0.07 | −0.78 | | – | – | – |

[a] These figures refer to the compact peak of emission, and not the entire component

The radio window used for the calculation of $L_{tot}$ was bounded at the lower frequencies (for $A_1$) by the expected self-absorption cutoff, and at high frequencies (for $B_1$ and $B_2$) by the onset of severe spectral steepening (~15 GHz). The usual assumptions of cylindrical geometry, unity filling factor, equipartition of energy between fields, electrons, and protons, random pitch angle distribution etc. were used in the calculation of $U_{min}$ and $T_{synch}^{5000}$ (synchrotron lifetime at 5 GHz)

telescopes, and a continuous period of ~18 h. Because of the relatively large overall extent of the source, it was necessary to use an integration time of only 1 min in order to achieve adequate sampling of the visibility function, and as a result the signal to noise ratio in each integration was poor, especially on the intrinsically less sensitive long Defford baselines. The use of closure phase in the mapping technique (Cornwell and Wilkinson, 1981) mean that the phase noise on these long baselines was, to a certain extent, propagated throughout the corrected data set, with the result that the flux density of the components on the map was underestimated, despite the reliability of the structure itself. This effect is most severe for the northern hotspot, and we present a map of this feature which was made without Defford in the data set. The lower surface brightness parts of the southern hotspot are not well represented on the map made with Defford, despite the effective weighting down of these baselines by the use of a 0.″10 restoring beam (compared to the theoretical beamsize of 0.″085), and so we also include a map of this feature made without Defford. These maps are shown in Figs. 2a–c.

The various components are labelled in the diagrams, and their measured and derived properties are given in Table 1.

These observations at 6 and 18 cm show 3C205 to possess a number of interesting features, which are listed below.

(i) The peaks of emission in the northern hotspot, the core, and the southern hotspot lie in a straight line to within the accuracy of our measurements (see Fig. 1). The distance from the core to the line joining the two hotspots is less than 1/400 of the separation of the hotspots. In other words seen from the core the two hotspots are in position angles separated by $179.^{\circ}9\pm0.^{\circ}2$. By present standards, this degree of alignment is extraordinary.

(ii) On the 1666 MHz map, the flat spectrum core component appears to be slightly elongated along a position angle some 15° greater than that of the source axis. The lack of such an elongation at 5 GHz may be a spectral effect, but confirmation of this is required. We will proceed on the assumption that the elongation exists, and is misaligned with the source axis.

(iii) The peak of the southern hotspot $A_1$ is unresolved in the transverse direction, and so has an angular size of less than ~50 milliarcsec (250 pc). In spite of this small size, it is extremely luminous, accounting for approximately one third of the total source flux density at 1666 MHz.

(iv) There is a pronounced tail of emission extending back towards the quasar from $A_1$ along the source axis, for a distance of ~0.″2 (1 kpc) (see Fig. 2b).

(v) The southern hotspot complex $A_1+A_2$ shows a pronounced zig-zag morphology, with a ridge starting at $A_1$ and leading to

**Table 2.** Parameters of the VLB interferometer array

| Telescope | Diameter (m) | $T_{sys}$ (K) | $T_0$ (K Jy$^{-1}$) | Freq. standard |
|---|---|---|---|---|
| Effelsberg (FRG) | 100 | 57 | 1.47 | H-maser |
| Dwingeloo (NL) | 25 | 35 | 0.11 | Rubidium |
| Jodrell Bank (UK) | 76 | 89 | 0.8 | Rubidium |
| Onsala (S) | 25 | 23 | 0.09 | H-maser |

the peak of $A_2$. This ridge can be clearly seen close to $A_1$ in Figs. 1b and 2a and becomes quite faint further away from $A_1$. From the peak of $A_2$ the ridge line turns sharply west, curves through $\sim 90°$ to a secondary peak, and continues to the SE, decreasing in surface brightness until disappearing into the noise. The total length of this curving ridge is about 3.″5 ($\sim$17 kpc).

(vi) The northern lobe consists of two distinct components $B_1$ and $B_2$. The bright hotspot $B_1$ has a sharp leading edge oriented in position angle $\sim 120°$ and approximately 0.″3 (1.5 kpc) in length. There is a fairly well defined peak of emission in the middle of this ridge. Behind the edge, the surface brightness falls off slowly towards the quasar for a distance of $\sim$0.″5 (2.5 kpc). Component $B_2$ is a relatively diffuse, very steep spectrum region of emission some 1.″5 (7.5 kpc) back towards the quasar from the leading edge of $B_1$.

### 2.2. *European* VLBI *Network* (EVN) *observations*

In addition we have also observed 3C205 with four telescopes of the EVN at 1612 MHz using the standard MK II C technique (Clark, 1973). Table 2 gives the relevant telescope parameters. The lobe spacings for the interferometers range from about 0.″15 to 0.″04. These observations were made on April 17/18 1982. Correlation of the data was carried out at the Max-Planck-Institut für Radioastronomie, Bonn, West Germany, and the source was clearly detected on all baselines, as expected (Barthel, 1983). After determining coherence losses we integrated the correlation coefficients for 6 min, with the phase centre on the ultra compact southern hotspot. The correlated flux densities were next calibrated according to Cohen et al. (1975) assuming the primary calibrator OQ 208 to be unresolved on all baselines, with a flux density of 1.02 Jy. The resulting hybrid map of the southern hotspot is reproduced in Fig. 3. This map has been made with a circular gaussian restoring beam of FWHM 0.″025. The ridgeline in the hotspot is found to bend through an angle of approximately 45° from north to south-east, although most of the flux density originates to the south of this bend. The hotspot is unresolved in the transverse direction (<15 milliarcsec).

## 3. Discussion

### 3.1. *The source linearity*

Before discussing the consequences of an intrinsic alignment of the source to within 0.°3, we must note the possible effects of projection on the observed bend angle. A source with an intrinsic bend angle $\theta$ is more likely to have an apparent bend angle $\theta_{app} < \theta$ than $\theta_{app} > \theta$, so that the intrinsic bend angle in 3C205 is, in the absence of prior information as to the orientation of the source, probably somewhat larger than the observed angle. Since 3C205 is of relatively large angular extent for a redshift of 1.5, the source axis is probably not close to the line of sight, so there is roughly a 15% chance that our upper limit for the observed bend angle of 0.°3 corresponds to 1° or more in the source. Some of the arguments to follow are, to first order, independent of projection effects. It will however henceforward be assumed that the intrinsic bend angle is of order 0.°3 as measured, since for 3C205 such an alignment is at least suggested by the data instead of being virtually ruled out by a relatively large observed misalignment as in other sources.

A brief comment on the statistics of gravitational lenses is now appropriate. 3C205 has a redshift of 1.534, and so a priori one would expect a relatively high surface density of objects capable of producing significant gravitational distortion of the radio structure. Ordinarily, any such distortion would be swamped by the intrinsic bends present in most sources, but in the case of 3C205 we can say that there are no foreground galaxies or clusters close enough in the sky to produce a bend of >0.°3, independent of projection effects. Blandford and Jaroszyński (1981) showed that the rms bend angle of triple sources is a calculable function of the angular size of the source and the mean density of clustered matter in the universe $\bar{\Omega}$ [their Eq. (19)]. For sources of 17″ size and redshift 1.5, the rms bend angle should be $\sim 10° \bar{\Omega}$. Clearly, further observations of high redshift, straight sources such as 3C205 will put interesting upper limits on $\bar{\Omega}$.

The linearity of this source is one of its most striking features, and, with some reservations about projection effects, allows us to set useful constraints on the collimation and ejection mechanisms in the quasar itself, as well as on the interaction of the ejected material with the external environment. By adopting the conventional view of the generation of radio sources by ejection of material from the nucleus of an active galaxy, we may deduce that the source axis in 3C205 is fundamentally and accurately defined within a relatively short distance of the nucleus itself. If instead the ejecta on the two sides were misaligned out to distances of tens of kpc, then something would be required to deflect these ejecta back "on course" by different, but precisely determined amounts. This implies the presence of an object of great inertia and of size tens of kpc, which possesses an axis of symmetry defined to within 0.°3. The outer reaches of even the most massive galaxy are too tenuous and lack the inertia to accurately deflect ejecta which transmit power at the rate of $\sim 10^{45}$ erg s$^{-1}$ to the outer lobes. In any case, there is no known example of a galaxy which clearly displays an axis of symmetry defined to such accuracy in the outer regions.

Conversely, if the ejection axis is defined deep within the nucleus of the galaxy, say in an accretion disc (Lynden-Bell, 1978) or a flattened disc of gas on scales of a few parsecs (Wiita, 1978), this axis can be determined by the average angular momentum direction of material accreted from the outer reaches of the galaxy, or even by the angular momentum direction of the central massive black hole (Rees, 1978). In this case, the stability of the axis could be extremely good. What is perhaps more surprising is the apparent ability of the ejecta to propagate through the central regions of a quasar, characterised by dense, rapidly moving clouds of gas, without being significantly deflected. This suggests a zone in the quasar in which things are relatively undisturbed. Such models have been proposed in the past to account for the statistical properties of broad and narrow line radio galaxies (e. g. Osterbrock, 1979).

A second way of obtaining accurate alignment is to postulate a well defined mean direction about which the ejection axis is allowed to wander on short timescales. If the hotspot location depends on the behaviour of the ejecta averaged over a relatively

long period, such alignment could result. A model of this type, involving subrelativistic ejection and accumulation of mass and momentum in the outer lobe (Lonsdale and Morison, 1983) is discussed in Sect. 3.3. First, however, we consider the constraints upon the standard beam model (Blandford and Rees, 1974, 1978) set by our observations.

### 3.2. *The beam model*

(i) General

We consider a standard beam model, wherein a continuous steady collimated flow of material with a speed $V_j$ propagates away from the nucleus until striking the external medium at a working surface and generating a hotspot. We will ignore the fact that the northern and southern lobes are extremely dissimilar, and consider only the southern lobe as the product of a currently active beam. The radius of the jet at the hotspot $r_j$ cannot be larger than the hotspot, so we set $r_j = 75$ pc. The jet must supply all the power radiated by the hotspot $A_1 \sim 3\,10^{44}$ erg s$^{-1}$, with a characteristic efficiency $\varepsilon < 1$. Assuming that the jet material is completely decelerated to the hotspot velocity at the working surface, the internal pressure of the hotspot must equal the momentum flux per unit area flowing down the jet in the hotspot rest frame. It is now a simple matter to show that for a given value of the energy flux down the jet, there is a minimum momentum flux into the hotspot, and that the balance condition at the hotspot thus yields a lower limit on $\varepsilon$ (e.g. Barthel and Lonsdale, 1983). For the southern lobe of 3C205, this value for $\varepsilon$ is 0.4 corresponding to a highly relativistic jet. The implied value of $\varepsilon$ rises if the hotspot is found to emit energy in other wavebands, or if the radius of the hotspot is shown to be smaller than 75 pc. $\varepsilon$ reaches unity at a flow speed $V_j \simeq 0.6c$. The above calculations are not very sensitive to $H_0$. Thus a beam model is only viable for 3C205 providing the jet is at least mildly relativistic, and providing the bulk kinetic energy of the jet is converted at nearly unit efficiency into relativistic electron and magnetic field energy. What is more, the dominant energy loss mechanism in the southern lobe must be synchrotron radiation (this is reasonable, given the synchrotron lifetime of $< 10^3$ yr, see Table 1). The waste energy problem alluded to by Rees et al. (1981) for relativistic jets is ameliorated, but only at the expense of severe constraints on energy conversion mechanisms. The standard beam model becomes untenable if we require the beam to supply the power for the entire southern lobe ($8\,10^{44}$ erg s$^{-1}$), unless the hotspot is not in equipartition, thereby raising the internal energy density of the hotspot.

(ii) Alignment

The overall alignment of the source, and apparent misalignment of the core set useful constraints on the degree of stability of the ejection axis due to the nature of the hotspot formation mechanism. Identifying the hotspot as the working surface of a narrow beam (Blandford and Rees, 1974) and allowing the ejection direction to vary at an angular rate $\omega$, the observed alignment implies $\omega \lesssim^{-7}$ rad yr$^{-1}$, assuming that the overall source axis lies $\gtrsim 15°$ from the plane of the sky. This is not a severe constraint, compared to the values one can deduce from long straight jets such as the one in NGC 6251 (Saunders et al., 1981), which may be $10^{-8}$ or even $10^{-9}$ rad yr$^{-1}$. However, on the assumption that this angular speed $\omega$ is constant, and identifying the $\sim 15°$ misalignment of the core component with a misalignment of the ejection axis we can infer a maximum of $c/20$ for the ejection velocity. Since we have shown this ejection speed to be inconsistent with a standard beam model for this source, either the core misalignment reflects a sudden change in the source axis (a "glitch") or its identification with the actual ejection axis is wrong. A consequence of the first possibility is that, in order to avoid the conclusion that our observations have been fortuitously timed, the beam must be able to propagate many kiloparsecs in the new direction, without generating radio emission.

(iii) Hotspot and lobe characteristics

In a conventional beam model, the internal pressure of the hotspot is balanced by the ram pressure of its advance into the external medium. Statistical evidence suggests that the rate of advance $V_h$ is typically $0.2c$ or less (Longair and Riley, 1979; Macklin, 1981), and using the energy density for $A_1$ in Table 1b we deduce an external medium number density of at least $6\,10^{-3}$ cm$^{-3}$. This is rather high compared to estimates of cluster medium densities from X-rays (Forman et al., 1981), and varies as $V_h^{-2}$.

An argument against the hotspot being in ram-pressure balance with the external medium arises from the apparent morphological link between this feature and the much more diffuse $A_2$. As can be seen in Figs. 1b, 2a, and 3 there is a definite extension away from the compact peak in the direction of the brightest part of $A_2$. Also, the magnetic field in component $A_1$ is oriented in roughly the same direction as this extension. Both these facts suggest that component $A_2$ is generated by outflow of material from $A_1$, with the peak of $A_2$ being a secondary "working surface". A possible cause of such outflow is the formation of an oblique shock in the beam at $A_1$, causing a deflection in the flow pattern towards $A_2$. The major part of the beam momentum would be deposited at $A_1$ so that strong magnetic fields and synchrotron emission might be expected immediately after the shock. If instead $A_2$ was formed directly by the beam at a time when it pointed in a different direction, it must be unpowered now, and it is thus difficult to explain why electrons are still able to radiate at 15 GHz [$\sim 40$ GHz in the source frame – Laing (1981)]. Spectral steepening is already pronounced in the northern lobe, which according to this idea must have been formed after $A_2$. A characteristic of the relativistic beam model is the rapid decay of luminosity which follows removal of the power input to a lobe (Lonsdale and Morison, 1983), yet $A_2$ actually radiates more power than the currently active $A_1$. The present observations strongly suggest that $A_2$ is a by-product of current activity rather than a relic of previous activity.

Clearly, given the outflow hypothesis, the hotspot $A_1$ must remain in approximately the same position long enough to generate $A_2$. The total minimum internal energy contained in $A_2$ is $\sim 8\,10^{58}$ erg. According to the calculations in Sect. 3.1(i), the jet cannot be supplying more than $\sim 2.5\,10^{45}$ ergs$^{-1}$ to the outer lobe at the present time. At this rate, even assuming negligible energy losses during the various stages of energy transport, and ignoring synchrotron losses in $A_2$ ($t_{\rm synch} \sim 5\,10^5$ yr at 1666 MHz), it would take at least $10^6$ yr to build up $A_2$. 3C205 is one of the most luminous sources in the sky, so it seems unlikely that the jet was significantly more powerful in the past. During the $10^6$ yr required for the formation of $A_2$, $A_1$ cannot have moved more than $\sim 5$ kpc ($1''$) because of the morphological link, and we deduce an upper limit to $V_h$ of $\sim 0.016c$. Ram pressure confinement of $A_1$ with this value of $V_h$ implies an external medium density of at least 1 particle cm$^{-3}$. If such a dense medium were uniform and hot ($5\,10^7$ K), the X-ray luminosity of 3C205 would be at least one order of magnitude higher than that observed (Feigelson and Berg, 1983; Zamorani et al., 1981), and the diffuse features $B_2$ and $A_2$ would be in a state of collapse, due to the high external static pressure. Thus,

if $A_2$ is really generated by outflow from $A_1$, the conventional beam model requires that $A_1$ be embedded in a dense filament of relatively cool gas. From this one might predict an association of optical line emission with the southern lobe of 3C205.

To summarise the constraints on the conventional beam model of radio sources set by these observations:

(a) The beam must be at least mildly relativistic, and conversion of energy to radio emission must be $>40\%$ efficient.

(b) The mean apparent rate of change of direction of the ejection $\omega < 10^{-7}$ rad yr$^{-1}$, unless the source axis is very close to the plane of the sky.

(c) If the core is genuinely misaligned by 15° and this misalignment is identified with the nuclear ejection axis, this represents a relatively sudden change in the axis. A consequence is that the beam must be able to propagate over a long distance without generating radio emission.

(d) The hotspot is unlikely to be confined by ram pressure of advance into a uniform external medium, due to its high minimum internal energy density. If the secondary component $A_2$ is fuelled by outflow from the hotspot $A_1$, a hypothesis which has observational support, then the only way to achieve ram pressure balance is to postulate dense cool clouds of gas with small filling factor $>40$ kpc from the active nucleus.

### 3.3. *Plasma cloud model*

(i) General

The multiple plasmoid model was first proposed by Christiansen (1973), developed by Christiansen et al. (1977), and discussed in a slightly modified form by Lonsdale and Morison (1983). The latter paper concerned the observations of sources which appeared different on the two sides of the nucleus, in that one side appeared active and possessed a very compact hotspot whilst the other appeared more relaxed, had a steeper spectrum, and a larger hotspot. It was argued that a natural interpretation of this asymmetry was that the "active" lobe was currently being powered, whilst the diffuse lobe was not, and that in order to maintain the observed luminosity of the diffuse lobe it was necessary to postulate a large, perhaps invisible, massive plasma cloud built up during an active phase, whose bulk kinetic energy was later tapped via instabilities and turbulent particle acceleration. In this model, it is possible to account for the extreme compactness of the active hotspots by identifying them with vigorous Rayleigh-Taylor instabilities at the leading edge of the cloud (Christiansen et al., 1977). They are thus regarded as transient features. 3C205 displays the same form of asymmetry as the sources investigated by Lonsdale and Morison, as well as an ultracompact hotspot in the southern lobe. The hotspots $A_1$ and $B_1$ are clearly separated into class I and class II in the proposed Lonsdale and Morison scheme.

Because of the energy storage properties of the massive plasma cloud which accumulates in the lobe, the luminosity of the hotspot depends only on the details of the energy conversion process in the instability, and so no straightforward constraints on the ejection speed, power and efficiency (as in the beam model) are possible.

(ii) Alignment

In this model the alignment of the source sets constraints more effectively on the hotspot formation processes in the outer lobe than on the central collimating mechanism itself. This is because the hotspot position may be thought of as an average of the ejection direction over a timescale related to the build up of the massive plasma cloud. The ejection axis can be allowed to wander over a much shorter timescale than this, whilst the hotspot location is cushioned by the presence of the plasma cloud.

Consider the hotspot formation process at the leading edge of the proposed plasma cloud. The cloud is likely to subtend a large angle as seen from the nucleus (Longair et al., 1973), and may be typically 15 kpc in diameter. The radius of curvature $r$ of the front of the cloud will thus be of order 5 kpc, and so the location of the hotspot is apparently defined to within 3% of this radius of curvature. The variation in the angle that the plasma cloud surface makes with the direction of motion over this range is about 3%, so this factor alone is unlikely to be sufficient to suppress the formation of a hotspot off-axis. A physical feature that could be defined to this accuracy is the stagnation point in the post-shock flow around the cloud. As Christiansen et al. (1977) pointed out, the growth of instabilities is effectively suppressed by the convective action of the bow shock flow, which sweeps newly developed instabilities away round the sides before they reach significant size. The compactness of the hotspot $A_1$ implies that the instability wavelength $\lambda$ is close to the minimum value of $0.01r$ for which significant growth can occur. Close to this limit, large amplitude instabilities are convected away quickly, and it seems likely that the conditions necessary for the formation of compact features such as $A_1$ depend strongly on the tangential component of the shocked flow, thus rendering the stagnation point the only location with such favourable conditions. Longer wavelength instabilities are likely to be less localized, because the growth timescale $\tau$ varies as $\lambda^{1/2}$, whilst the convection decouples the instability from the plasma cloud in a time $t_{dc} \alpha \lambda$.

If this argument is valid, and the location of the hotspot is determined by the position of the stagnation point, we can infer constraints upon the symmetry of the bow shock flow. The external medium must be homogeneous on size scales of up to a few kpc, otherwise significant distortion of the hypersonic flow pattern would be expected. This model is thus consistent with, and to a certain extent requires, an external medium which is tenuous and hot ($n \sim 10^{-4}$ cm$^{-3}$, $T \sim 5\,10^7$ K would be reasonable numbers, for which approximate static pressure balance of the most diffuse features holds). The stagnation point occurs along the line passing through the centre of the plasma cloud, and directed along the velocity vector of the cloud relative to the external medium, assuming homogeneity. This velocity vector is in the same direction in the two lobes to within $\sim 1°.5$, assuming a cloud radius $\sim 5$ kpc. The allowed magnitude of the random fluctuations in the momentum vector of the cloud $\Delta M$ are thus $\sim 0.03M$, where $M$ is the cloud momentum. Suppose the central object ejects material into a cone of half angle $\sim 15°$ (as suggested by the core elongation), with random variations in ejection direction within this core on a timescale $\Delta\tau$. The time taken for the cloud to form is denoted by $\tau$, and so we have

$$\frac{\Delta M}{M} \sim \frac{\Delta\tau}{\tau} \tan 15° < 0.03$$

or $\Delta\tau < 0.1\tau$. The direction of ejection must vary on a timescale faster than one tenth of the source lifetime, and such variations must be random in nature.

A second consequence of our 1°.5 tolerance on the direction of the relative velocity vector between the cloud and its surroundings is that the magnitude $\Delta v$ of large scale fluctuations in the velocity field (perpendicular to the line of sight) of the external medium which do not possess reflection symmetry through the position of the quasar, are required to be not more than $0.03v$, where $v$ is the

plasma cloud velocity. A likely value for $\Delta v$ in a cluster is $1000\,\mathrm{km\,s^{-1}}$, which gives $v > 0.12c$, but these values could be much lower if the parent galaxy is isolated (Longair and Seldner, 1979).

(iii) Hotspot and lobe characteristics

The identification of the feature $A_1$ with an instability raises the possibility that it is a transient feature, or explosion, of short duration. If this is true, the fact that such hotspots are common in high redshift sources (e.g. Barthel, 1983) argues that such explosions occur sufficiently often that at any given time the probability of a very compact feature being observable is high. From the map of 3C205 presented by Pooley and Henbest (1974) it is almost certain that a major part of the polarized flux at 5 GHz originates in $A_1$, and the polarization data (Tabara and Inoue, 1980) imply an internal sound speed for $A_1$ of $\sim c/\sqrt{3}$. Thus, even if the external medium were dense enough to significantly alter the symmetry of the explosion ($n > 0.03\,\mathrm{cm^{-3}}$) the hotspot would fade due to adiabatic expansion losses on a timescale of $\sim 300$ yr. In order to have a reasonable probability of being observed, these explosions must recur on timescales of a few thousand years or less.

If $A_2$ is the result of outflow from $A_1$ then we can infer that the hundreds of explosions necessary, on average, result in outflow in a well-defined direction and from a fairly definite location. Thus we deduce that the conditions necessary for producing the instability must be maintained for a time long compared to the growth or dissipation timescale of a hotspot. Furthermore, whatever defines the re-ejection axis must be associated with a long-lived structure possibly related to the massive cloud.

If the energy production in the hotspot is essentially continuous, we can show that the rate of adiabatic energy loss ($<$energy input to the hotspot) is of order $10^{47}\,\mathrm{erg\,s^{-1}}$, unless a very dense medium ($\geqq 1\,\mathrm{cm^{-3}}$) capable of significantly slowing the expansion speed is present. This is an uncomfortably high rate of energy supply, and incidentally also applies to the beam model if ram pressure balance does not hold. We have avoided this problem above by postulating that we are just a bit fortunate to catch the hotspot in a state of such rapid energy loss.

The hypothesis of collimated outflow of material $A_1$ to $A_2$ in either model requires confinement of $A_1$. If we regard $A_1$ as an explosive event triggered on a timescale of $< 10^3$ yr by an instability, differential ram pressure across the expanding hotspot caused by a density gradient can result in collimation. Even so, as discussed above, very high densities are required to affect the symmetry of the explosion, on the order of $0.1\,\mathrm{cm^{-3}}$. This is perhaps more reasonable for the cloud model than for the beam model, because in the former, the ejecta themselves are a potential origin of dense filaments, especially near the leading edge of the main plasma cloud. Also, in the cloud model there is no problem with maintaining the position of $A_1$ for the time required to generate $A_2$. Again, the suggested presence of a dense medium around $A_1$ implies that optical emission may be present.

To summarize the constraints on the plasma cloud model set by these observations

(a) The only obvious way of restricting the hotspot location to an accurately defined source axis is to postulate instability formation at the stagnation point. This is reasonable in view of current plasma cloud models.

(b) If the core misalignment is the result of a statistical fluctuation in the ejection direction, such fluctuations must occur on timescales of less than one tenth of the source lifetime.

(c) There cannot be any large scale inhomogeneities, in density or velocity field, of the external medium. Specifically, the plasma cloud speed must exceed $\sim 30$ times the velocity variations in this medium.

(d) Any hotspot formation mechanism must be able to 'remember' a re-ejection direction for $> 100$ times the dynamical timescales of the hotspot itself, on the hypothesis of collimated outflow of material from $A_1$ to $A_2$. As in the beam model, directing material from $A_1$ to form $A_2$ requires very high matter densities in the vicinity of $A_1$.

## Conclusions

The present data do not exclude either of the models considered here, but instead limit the range of properties of the ejection and the external medium allowed in each case. In the beam model, we deduce that the ejection velocity is high, the energy conversion efficiency is high, and set limits on how fast the ejection axis can alter its direction. A dense external medium is also required in the beam model. New constraints on the plasma cloud model include the maximum allowed timescale of fluctuations in the ejection direction (and hence a minimum frequency of ejection) and the homogeneity, in both density and velocity, of the external medium. In both models, the hypothesis of outflow from $A_1$ to $A_2$ requires very high densities of material in the vicinity of $A_1$, suggesting that a search for optical emission may be fruitful.

Further study of 3C205 promises even more stringest constraints on models. Confirmation of the core elongation with VLBI is necessary. The inferred dense medium surrounding $A_1$ should produce obvious polarization structure on the 0.″1 scale, with significant polarization being present only after the flow has been recollimated (i.e. in the structure elongated in position angle $\sim 140°$). The possibility of still more compact structure in $A_1$ is of interest, and may lead to the eventual feasibility of a direct measurement of relative motion between $A_1$ and the core. The detection of line emission from $A_1$ may also give this information, since the confining material could be co-moving with the hotspot. One way to distinguish between the models presented here would be to make very sensitive observations in order to detect either a jet, or evidence of a large plasma cloud. Finally, it may be of interest to some that had these observations been made in 1974, the gravitational slingshot theory of extragalactic radio sources (Saslaw et al., 1974) would have enjoyed the advantage of an ideal prototype source, and would thus have commanded greater popularity. The extreme alignment, VLBI scale hotspot, and misaligned core elongation are all natural consequences of such a model.

*Acknowledgements.* We thank Drs. I. W. A. Browne, G. K. Miley, C. A. Norman, R. H. Sanders, R. T. Schilizzi as well as Prof. H. van der Laan for comments and discussions. CJL acknowledges receipt of an SERC postdoctoral research fellowship. PDB acknowledges support by the Netherlands Foundation for Astronomical Research (ASTRON) with financial aid from The Netherlands Organization for the Advancement of Pure Research (ZWO). PDB also acknowledges travel support from the Leids Kerkhoven-Bosscha Fonds.

## References

Barthel, P.D.: 1983, *Astron. Astrophys.* **126**, 16
Barthel, P.D., Lonsdale, C.J.: 1983, *Monthly Notices Roy. Astron. Soc.* **205**, 395

Barthel, P.D., Lonsdale, C.J.: 1984 (in preparation)
Blandford, R.D., Jaroszyński, M.: 1981, *Astrophys. J.* **246**, 1
Blandford, R.D., Rees, M.J.: 1974, *Monthly Notices Roy. Astron. Soc.* **169**, 395
Blandford, R.D., Rees, M.J.: 1978, *Physica Scripta* **17**, 265
Christiansen, W.A.: 1973, *Monthly Notices Roy. Astron. Soc.* **164**, 211
Christiansen, W.A., Pacholczyk, A.G., Scott, J.S.: 1977, *Nature* **266**, 593
Clark, B.G.: 1973, *Proc.* IEEE **61**, 1242
Cohen, M.H., Moffet, A.T., Romney, J.D., Schilizzi, R.T., Shaffer, D.B., Kellermann, K.I., Purcell, G.H., Grove, G., Swenson, Jr., G.W., Yen, J.L., Pauliny-Toth, I.I.K., Preuss, E., Witzel, A., Graham, D.: 1975, *Astrophys. J.* **201**, 249
Cornwell, T.J., Wilkinson, P.N.: 1981, *Monthly Notices Roy. Astron. Soc.* **196**, 1067
Davies, J.G., Anderson, B., Morison, I.: 1980, *Nature* **288**, 64
Feigelson, E.D., Berg, F.: 1983, *Astrophys. J.* **269**, 400
Forman, W., Bechtold, J., Blair, W., Jones, C.: 1981, in X-*Ray Astronomy with the Einstein Satellite*, ed. R. Giacconi, Reidel, Dordrecht, p. 187
Kapahi, V.K., Schilizzi, R.T.: 1979, *Nature* **277**, 610
Laing, R.A.: 1981, *Monthly Notices Roy. Astron. Soc.* **195**, 261
Longair, M.S., Riley, J.M.: 1979, *Monthly Notices Roy. Astron. Soc.* **188**, 625
Longair, M.S., Seldner, M.: 1979, *Monthly Notices Roy. Astron. Soc.* **189**, 433
Longair, M.S., Ryle, M., Scheuer, P.A.G.: 1973, *Monthly Notices Roy. Astron. Soc.* **164**, 243
Lonsdale, C.J., Morison, I.: 1983, *Monthly Notices Roy. Astron. Soc.* **203**, 833
Lynden-Bell, D.: 1978, *Physica Scripta* **17**, 185
Macklin, J.T.: 1981, *Monthly Notices Roy. Astron. Soc.* **196**, 967
Osterbrock, D.E.: 1979, *Astron. J.* **84**, 901
Pooley, G.G., Henbest, S.N.: 1974, *Monthly Notices Roy. Astron. Soc.* **169**, 477
Rees, M.J.: 1978, *Nature* **275**, 516
Rees, M.J., Begelman, M.C., Blandford, R.D.: 1981, *Annals New York Acad. Sci.* **375**, 254
Robson, D., Lonsdale, C.J., Stannard, D.: 1984 (in preparation)
Saslaw, W.C., Valtonen, M.J., Aarseth, S.J.: 1974, *Astrophys. J.* **190**, 253
Saunders, R., Baldwin, J.E., Pooley, G.G., Warner, P.J.: 1981, *Monthly Notices Roy. Astron. Soc.* **197**, 287
Schmidt, M.: 1968, *Astrophys. J.* **151**, 393
Tabara, H., Inoue, M.: 1980, *Astron. Astrophys. Suppl.* **39**, 379
Wiita, P.J.: 1978, *Astrophys. J.* **221**, 41
Wyndham, D.: 1966, *Astrophys. J.* **144**, 459
Zamorani, G., Henry, J.P., Maccacaro, T., Tananbaum, H., Soltan, A., Avni, Y., Liebert, J., Stocke, J., Strittmatter, P.A., Weymann, R.J., Smith, M.G., Condon, J.J.: 1981, *Astrophys. J.* **245**, 357